

# Demonstration of quantum-limited discrimination of multi-copy pure versus mixed states

Arunkumar Jagannathan<sup>1</sup>, Olivia Brasher<sup>2</sup>, Michael Grace<sup>3</sup>,  
Jeffrey H. Shapiro<sup>4</sup>, Saikat Guha<sup>3</sup>, and Jonathan L. Habif<sup>1,2</sup>

<sup>1</sup> *Information Sciences Institute, University of Southern California, Waltham, MA 02451*

<sup>2</sup> *Ming Hsieh Department of Electrical and Computer Engineering,  
University of Southern California, Los Angeles, CA 90089*

<sup>3</sup> *James C. Wyant College of Optical Sciences, University of Arizona, Tucson, AZ 85721* and

<sup>4</sup> *Research Laboratory of Electronics, Massachusetts Institute of Technology, Cambridge, MA 02139*

(Dated: June 17, 2022)

We provide a demonstration of an optical receiver that achieves the quantum Chernoff bound for discriminating pure coherent laser states from thermal states. We find that the receiver approaching the Helstrom bound, for single-copy measurement for this discrimination task, is sub-optimal in the multi-copy case. We also provide a theoretical framework proving that, for a large class of discrimination tasks between a pure and a mixed state, any Helstrom-achieving receiver is sub-optimal by a factor of at least two in error exponent compared to a receiver that achieves the quantum Chernoff bound.

A revolution in the fields of sensing and metrology is underway with new insights about how a complete quantum mechanical description of a sensing system and the fields to be sensed can reveal fundamental bounds to the achievable sensitivity of a sensor. These fundamental bounds can far exceed that achievable with a classical treatment of the physical configuration. Sensing can be coarsely categorized into two modalities: *parameter estimation* where the task is to determine the value of a continuous parameter (e.g. distance, phase, velocity) with minimized variance on the estimate, and *state discrimination* where the task is to identify the value of a parameter when a finite number of possibilities exist (e.g. direction of rotation, number of targets in a cluster).

A wealth of work has been dedicated to quantum-limited single-copy state discrimination in the context of discriminating symbols in a photon-starved classical communications link. Nearly the entirety of these investigations have focused on discriminating between quantum pure states (such as laser states) that make up a constellation for a communications symbol. Receivers that approach or achieve the Helstrom bound, which sets the ultimate achievable average error probability for quantum state discrimination, have been proposed and demonstrated for the cases of constellations of coherent states of size  $N = 2$  [1–5], and  $N > 2$  [6–10]. These quantum measurements all follow a general architecture of coherent displacement of the received pure state followed by photon-counting. Interestingly, this same quantum measurement prescription was proposed in [11] for achieving optimal discrimination for *multi-copy* quantum states proving that such a receiver can achieve the quantum Chernoff error exponent [12].

More recently, investigations have examined discrimination between a broader class of quantum states to include mixed states [13–17]. Experimental work has demonstrated techniques for improved discrimination be-

tween single-copy pure and mixed quantum states [18] including a demonstration that approached the Helstrom bound [19]. Little work, experimental or theoretical, has been done investigating the quantum limits to discrimination of multi-copy pure versus mixed states.

In this Letter we present the first experimental demonstration of a receiver discriminating non-orthogonal quantum optical states at the quantum Chernoff bound (QCB). Over a broad range of received optical intensities we show that the Kennedy receiver [4], traditionally reserved for optical phase-encoded symbol discrimination in a communications setting, can be applied to discriminate thermal and coherent states at the QCB. Moreover, we show experimentally that the receiver that approaches the Helstrom bound for the same single-copy discrimination problem is strictly sub-optimal for achieving quantum-limited sensitivity when measuring over many copies of the quantum state, and we theoretically prove that the sub-optimality of the Helstrom-achieving measurement holds for all discrimination tasks between pure and mixed states that obey a broadly applicable symmetry condition.

In a single spatio-temporal polarization mode, a coherent state generated by a shot-noise limited laser with mean photon number  $\bar{n} = |\alpha|^2$  is expressed as a density operator  $\rho_{\text{coh}} = |\alpha\rangle\langle\alpha|$ . The density matrix for a corresponding thermal state with the same average intensity is written as  $\rho_{\text{th}} = \sum_{n=0}^{\infty} \frac{\bar{n}^n}{(\bar{n}+1)^{n+1}} |n\rangle\langle n|$ , where the index  $n$  represents the photon number (Fock) basis. We aim to discriminate between  $M$  copies from sources generating these two types of states  $\rho_R \in [\rho_{\text{coh}}, \rho_{\text{th}}]$ , such that the total state available to the receiver will be one of the two candidate tensor product states  $\rho_R^{\otimes M} \in [\rho_{\text{coh}}^{\otimes M}, \rho_{\text{th}}^{\otimes M}]$  with equal *a priori* probabilities. To quantify receiver performance, we use the average error probability  $P_{\epsilon}^{(M)} = (1/2)[P(\rho_{\text{coh}}^{\otimes M} | \rho_{\text{th}}^{\otimes M}) + P(\rho_{\text{th}}^{\otimes M} | \rho_{\text{coh}}^{\otimes M})]$  as a metric, which averages the conditional error probabil-

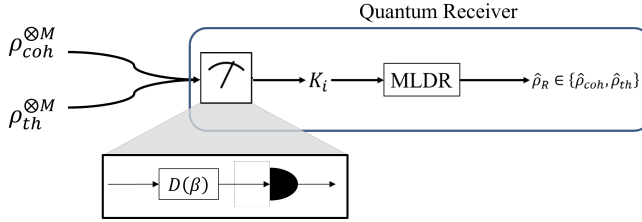


FIG. 1. Schematic of the persistent sensing quantum-limited discrimination scenario. Two candidate persistent sources are equi-probably in arrival at the receiver. A quantum measurement apparatus makes measurements on each of the  $M$  arriving states and uses those measurement results in a maximum likelihood decision rule (MLDR) to make a decision about which source generated the received states.

ity of the receiver making the decision  $\rho_R^{\otimes M}$  of an  $M$ -mode coherent state when the true state  $\rho_R^{\otimes M}$  was from the thermal state source and vice versa. As  $M \gg 1$ , the error probability for discrimination obeys the upper bound  $P_\epsilon^{(M)} \leq \frac{1}{2} \exp(-\xi^{\text{Meas}} \cdot M)$ , where  $\xi^{\text{Meas}}$  is known as the Chernoff exponent for a particular measurement [20]. Quantum mechanics bounds this asymptotic error decay rate via the quantum Chernoff bound  $\xi^{\text{Meas}} \leq \xi^{\text{QCB}}$ , where the quantum Chernoff exponent  $\xi^{\text{QCB}} = -\ln(\min_{0 \leq s \leq 1} \text{Tr}[\rho_{coh}^s \rho_{th}^{1-s}])$  maximizes the Chernoff exponent over all physically allowed measurements of the state  $\rho_R^{\otimes M}$  [12, 21]. As illustrated in Fig. 1, a receiver is comprised of a quantum state measurement followed by processing of the measurement results through a maximum likelihood decision rule (MLDR) resulting in a decision about which state was received. The most general receiver would make an optimal joint measurement over all  $M$  copies of the received state. In practice, finding an impelmenting an optimal joint measurement can be very difficult. However, when at least one of the states to be discriminated is a pure state, then joint measurements are not required to achieve the QCB. It is known ([22], *Theorem 6*) that a projection of all  $M$  copies of the received state onto the pure state, followed by post-processing of the measurement outcome of each copy, is sufficient for the quantum-optimal error decay rate, even though the single-copy average error probability  $P_\epsilon^{(1)} = (1/2)[P(\rho_{coh}|\rho_{th}) + P(\rho_{th}|\rho_{coh})]$  is not minimized. This procedure identifies the pure state with certainty, providing a sufficient statistic for the hypothesis test that minimizes the asymptotic error. The resulting attainable QCB for pure-vs-mixed state discrimination is given by  $\xi^{\text{QCB}} = -\ln(F(\rho_1, \rho_2))$ , where  $F(\rho_1, \rho_2) \equiv \text{Tr}[\sqrt{\sqrt{\rho_1} \rho_2 \sqrt{\rho_1}}]^2$  is the quantum fidelity between states with density operators  $\rho_1$  and  $\rho_2$  [22].

Our measurements in this work are composed of coherent linear optical displacement operations followed by a photon number resolving measurement, using photon number statistics to construct an MLDR for discrimina-

tion between the states. The displacement operator is  $\hat{D}(\beta) = \exp(\beta \hat{a}^\dagger - \beta^* \hat{a})$ , where  $\hat{a}^\dagger$  and  $\hat{a}$  are the standard quantum mechanical creation and annihilation operators, respectively. The QCB-attaining measurement can be implemented via a *Kennedy* receiver, where the state  $\rho_{coh}$  is displaced to the vacuum state  $|0\rangle\langle 0|$  [4]. When the vacuum state is measured with direct detection, it can be identified perfectly by noise-free direct detection yielding no photon counts, while a displaced thermal state will yield a photon detection signature. An alternative measurement scheme, a *Generalized Kennedy* (GK) receiver, displaces the state by a pre-computed amount to minimize  $P_\epsilon^{(1)}$  [1]. In both cases, we can use the photon counting statistics resulting from  $\hat{D}(\cdot)$  to compute the Chernoff exponents  $\xi^{\text{KEN}}$  and  $\xi^{\text{GK}}$  [20].

In [19] we presented an experimental demonstration of the Kennedy, GK and direct detection receivers for discriminating single-mode coherent and thermal state light. The experiments showed that the GK receiver closely approaches the Helstrom bound, while the Kennedy receiver was shown to be sub-optimal. Our work here shows both experimentally and analytically that the situation is reversed for multi-copy discrimination: the Kennedy receiver exactly attains the QCB, as expected [13, 22], whereas the GK receiver is decidedly not optimal by a provable factor.

The setup for experimental validation is shown in Fig. 2. A shot-noise limited 780 nm laser (Toptica DL100 Pro) generates continuous wave laser light providing source light for our experiment. Coherent states are directly derived from the laser source. Pseudo-thermal states are generated by taking a part of the laser beam, reflecting it off a rotating diffuser and recollecting the diffuse light in a single-mode optical fiber. The phase and am-

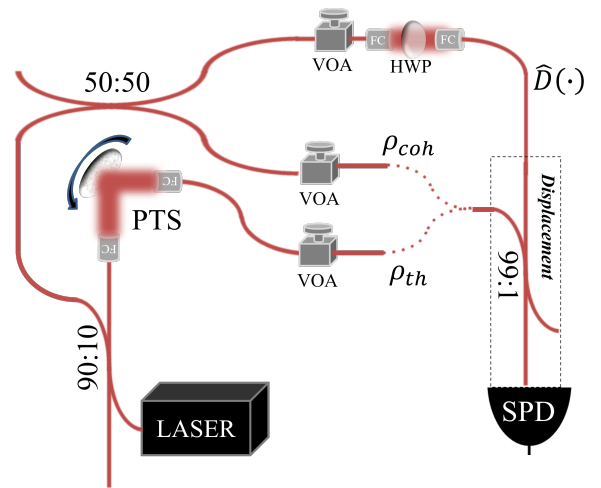


FIG. 2. Experimental Setup for multi-copy discrimination of mixed states. VOA: variable optical attenuator, PTS: pseudo-thermal source, HWP: Half-wave plate, SPD: single photon detector.

plitude of the reflected beam from the rotating diffuser varies randomly in time, reducing the temporal coherence to  $\sim 1\mu\text{s}$ . We measured the photon statistics of the psuedo-thermal state and verified that the photon statistics follows Bose-Einstein distribution [19]. In addition, we measured the second order correlation  $g^2(\tau) \sim 2$ , signaling the characteristic of a thermal state. The intensity of both the coherent state and the thermal state can be adjusted independently with a variable optical attenuator to generate a signal with mean photon number  $\bar{n}_S$ . The general architecture for the receivers, as illustrated in Fig. 1, involve a coherent displacement operation  $\hat{D}(\cdot)$  on the received state, followed by photon number resolving detection, which was implemented with a quasi-photon number resolving (qPNR) detector, described in [19] and in the supplement. The displacement operation is performed by harvesting a portion of the initial laser beam and mixing it with the signal state passing through a highly transmissive (99:1) beamsplitter. Following displacement, direct detection is performed with the qPNR detector on the resulting state and the photon counts are recorded. The experiment demonstrates three receiver implementations for discrimination: direct photon counting detection (DD), the generalized Kennedy (GK) receiver and the Kennedy (KEN) receiver. Each receiver is implemented by adjusting the amplitude of the displacement operation and each receiver achieves a unique error exponent for discriminating thermal and coherent state light, which varies as a function of signal strength. In the experiment a single copy of a quantum state is generated and detected within a time interval  $\tau = 1\mu\text{s}$ . Data is collected for  $T = 1\text{ ms}$  such that in each data collection cycle  $M = 1000$  copies of a state is generated by the source and detected by a receiver, resulting in 1000 measurement values.

For direct detection, the displacement amplitude is set to  $\hat{D}(\beta = 0)$ , and the signal beam is sent directly toward a quasi-photon number resolving (qPNR) detector (described in [19]) consisting of a photon-counting Si avalanche photodiode (Perkin Elmer SPCM-AQR-14) the electrical output of which is direct toward an oscilloscope for counting individual photon detects. The qPNR detector reports the number of detected photons  $n_D$  within each interval  $\tau$ . From the photon statistics for single mode coherent and thermal state light we can compute the conditional probabilities  $P^{\text{DD}}(n_D|\rho_R) = \langle n_D|\rho_R|n_D \rangle$  to construct the MLDR.

For the GK receiver, the displacement amplitude  $\hat{D}(\beta)$  is optimized for each value of signal intensity  $\bar{n}_S$  to minimize the single-copy measurement error probability  $P_\epsilon^{(1)}$ . The displaced state  $\hat{D}(\beta)\rho_R\hat{D}^\dagger(\beta)$  is directed to the qPNR detector for photon counting. Consistent with operation of the receiver for single-copy discrimination, in each mode we make a hard decision about the incoming received state deciding  $\rho_{\text{coh}}$  if  $n_D = 0$  and  $\rho_{\text{th}}$  otherwise. At the end of  $M$  measurements we compute the

fraction of outcomes for which  $\rho_{\text{coh}}$  was decided and set a threshold  $n^*$  for this fraction above which we make the final decision  $\rho_R^{\otimes M} = \rho_{\text{coh}}^{\otimes M}$ , and below which we decide  $\rho_R^{\otimes M} = \rho_{\text{th}}^{\otimes M}$ . To implement the MLDR, the threshold for this ratio is computed as,

$$n^* = \frac{\ln \left( \frac{1 - P^{\text{GK}}(0|\rho_{\text{coh}})}{1 - P^{\text{GK}}(0|\rho_{\text{th}})} \right)}{\ln \left( \frac{P^{\text{GK}}(0|\rho_{\text{th}})[1 - P^{\text{GK}}(0|\rho_{\text{coh}})]}{P^{\text{GK}}(0|\rho_{\text{coh}})[1 - P^{\text{GK}}(0|\rho_{\text{th}})]} \right)} \quad (1)$$

$$\text{where } P^{\text{GK}}(n_D|\rho_R) = \langle n_D|\hat{D}(\beta)\rho_R\hat{D}^\dagger(\beta)|n_D \rangle.$$

For the Kennedy receiver, the displacement amplitude  $\hat{D}(-\alpha)$  results in a state  $\hat{D}(-\alpha)\rho_R\hat{D}^\dagger(-\alpha)$  perfectly nulling the coherent state hypothesis, resulting in a vacuum state directed toward the qPNR detector, but generates a displaced thermal state when applied to  $\rho_{\text{th}}$  resulting in a mixed state with a Laguerre photon counting distribution [23]. In principle, a photon detection event in any of the  $M$  measurements results in a decision that  $\rho_R^{\otimes M} = \rho_{\text{th}}^{\otimes M}$ , where  $n_D = 0$  for all measurements assures that  $\rho_R^{\otimes M} = \rho_{\text{coh}}^{\otimes M}$ . In the ideal case, the Kennedy receiver saturates the QCB:

$$\begin{aligned} \xi^{\text{Ken}} &= \xi^{\text{QCB}} = -\ln(F(\rho_{\text{coh}}, \rho_{\text{th}})) \\ &= -\ln \left[ \frac{1}{1 + \bar{n}_S} \exp \left( -\frac{\bar{n}_S}{1 + \bar{n}_S} \right) \right]. \end{aligned} \quad (2)$$

In practice, the noise in our experimental setup results in a small deviation to the strict rule for the MLDR.

To make a decision about which state was received we use the sequence of measurements recorded by the receiver and apply an MLDR to the sequence of measurements. The MLDR is developed experimentally for each of the three receivers by collecting data and evaluating the photon detection statistics. This method for developing the MLDR naturally envelops non-idealities in an experimental setup such as dark counts in single photon detectors and background counts from ambient room lights (measured to be  $4 \cdot 10^{-4}$  counts per microsecond). Also, the experimental setup implemented has sub-unit detection efficiency owing to optical path losses and finite detection efficiency at the SPD. We characterized the overall receiver efficiency to be  $\eta_R = 0.45$ . We reference our experimental results against a normalized received optical intensity  $\bar{n}_R = \eta_R \bar{n}_S$ . In the Supplementary Material we quantify the impact of  $\eta_R$  on  $\xi^{\text{KEN}}$ .

For each value of  $\bar{n}_R$ , and for each receiver type, we have 1000 measurement results for each of the states presented to the receiver. To compute  $P_\epsilon^{(M)}$  we randomly select  $M$  measurements from the 1000 measurement results available and apply the MLDR to those  $M$  measurements resulting in a decision about which state was received. For each value of  $M$  this process is repeated up to 100 times to estimate the error probabilities  $P(\rho_{\text{coh}}^{\otimes M}|\rho_{\text{th}}^{\otimes M})$  and  $P(\rho_{\text{th}}^{\otimes M}|\rho_{\text{coh}}^{\otimes M})$ , which are used

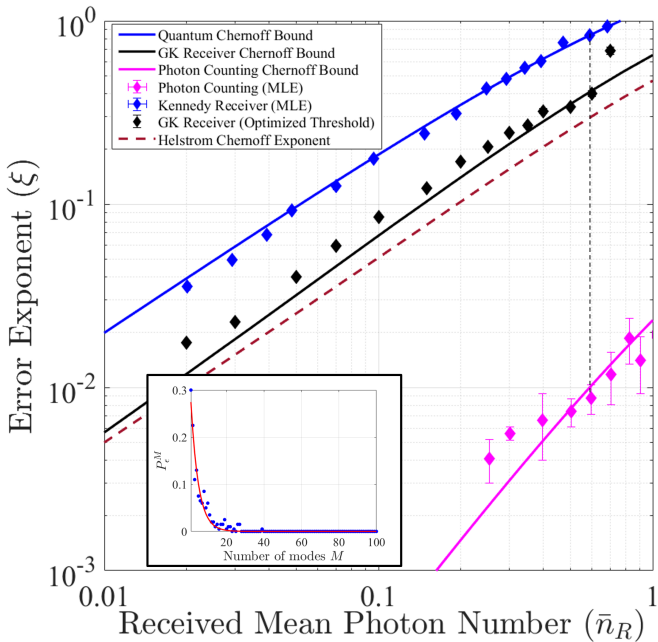


FIG. 3. Error exponent ( $\xi$ ) vs received mean photon number  $\bar{n}_R$ . Quantum Chernoff bound (Blue solid); Kennedy receiver experimental points (blue diamonds); GK receiver (black) Chernoff lower bound (solid line), experimental points (diamonds); direct detection (Magenta) Chernoff lower bound (solid line), experimental points (diamonds). Vertical black dashed line shows a factor of 100x in error exponent of the Kennedy receiver over the direct detection receiver. (Inset) An example of the calculated quantity  $P_\epsilon^{(M)}$ , along with an exponential fit used to extract the experimental error exponent.

to compute  $P_\epsilon^{(M)}$ . Fig. 3 (inset) shows the error probability  $P_\epsilon^{(M)}$  as a function the number of modes  $M$  for  $\bar{n}_R = 0.2$  for the Kennedy receiver (blue points). For all receivers, the error probability  $P_\epsilon^{(M)}$  decays exponentially with  $M$ . We determine an experimental error exponent  $\xi$  by doing an exponential fit (red solid line) of the form  $P_\epsilon^{(M)} = \frac{1}{2}[ae^{-\xi M}]$ , where  $a$  and  $\xi$  are free parameters. For each of the receivers the data collection and computation of  $P_\epsilon^{(M)}$  were repeated 5 times to estimate an uncertainty in the error exponents.

Fig. 3 shows the experimentally measured error exponent  $\xi$  as a function of the received mean photon number  $\bar{n}_R$  for all three receiver types. Comparing our results in Fig. 3 to the single mode measurements reported in [19], we see that the GK receiver, which is *nearly* optimal to achieve the ultimate Helstrom bound in the single-copy case, is not the optimal receiver to achieve the quantum Chernoff bound for multi-copy discrimination. Meanwhile, the Kennedy receiver, which was sub-optimal to achieve the Helstrom bound, achieves an error exponent in excellent agreement with the computed quantum Chernoff bound. At  $\bar{n}_R = 0.6$  the Kennedy re-

ceiver outperforms direct detection by approximately 20 dB in the experimentally observed error exponents. Our experimental data using the MLDR agree with the statistically computed Chernoff exponents ( $\xi^{\text{DD}}$ ,  $\xi^{\text{GK}}$ ,  $\xi^{\text{KEN}}$ ). For reference, we also plot the Chernoff exponent for the quantum measurement that is known to exactly saturate the Helstrom bound for single-copy state discrimination [24]. We observe that  $\xi^{\text{QCB}} > \xi^{\text{GK}} > \xi^{\text{Helstrom}}$ , with the quantum Chernoff bound (achieved by the Kennedy receiver) exceeding both  $\xi^{\text{GK}}$  and  $\xi^{\text{Helstrom}}$  by at least a factor of two. We also note that coherent homodyne detection, another common classical receiver, achieves a discrimination error exponent equal to that for the ideal Helstrom receiver, as shown in [13].

To make sense of the hierarchy of multi-copy receiver performance observed in Fig. 3, we analyze the Chernoff bound of a generalized measurement for an arbitrary state discrimination task between equiprobable quantum states  $\rho_1$  and  $\rho_2$ . In particular, we consider all decision schemes that act the same “copy-by-copy” measurement on each copy of the received state and perform a post-processing procedure (e.g., MLDR) that yields a hard decision following each copy. Such measurement schemes, which can be modeled by a two-element positive operator valued measure (POVM), induce a binary-input-binary-output statistical channel consisting of two possible single-copy outcomes associated with the two candidate states. Under this statistical model, the MLDR after  $M$  copies are processed reduces to thresholding on the single-copy outcomes [Eq. (1)]. In this setting, single-copy errors on the outcomes of individual copies can be tolerated in the effort to reduce the multi-copy discrimination error.

Consider a copy-by-copy measurement with a single-copy average error probability of  $P_\epsilon^{(1)} = (p+q)/2$ , where  $p = P(\rho_2|\rho_1)$  and  $q = P(\rho_1|\rho_2)$  are the conditional probabilities associated with the two types of incorrect decisions. We introduce a parameter  $b \in [-1, 1]$ , such that  $p = (1+b)P_\epsilon^{(1)}$  and  $q = (1-b)P_\epsilon^{(1)}$ , that quantifies the bias of the total average error toward either one type of conditional error or the other. In particular, the unbiased condition  $b = 0$  implies that the measurement induces equivalent conditional error probabilities  $p = q = P_\epsilon^{(1)}$ , indicating a Binary Symmetric Channel (BSC). In the Supplementary Material, we show that the Chernoff exponent  $\xi^{\text{Meas}} = -\ln(Q_{s_{\min}})$  for such a measurement can be evaluated by expanding  $Q_{s_{\min}}$  around  $b = 0$  to find

$$Q_{s_{\min}} = 2\sqrt{P_\epsilon^{(1)}(1 - P_\epsilon^{(1)})} - G(P_\epsilon^{(1)})b^2 + O(b^4), \quad (3)$$

where  $G(x)$  is a function defined in the Supplementary Material that is strictly positive on the domain  $x \in [0, 1/2]$ . Eq. (3), which holds even when both candidate states are mixed, can be used to find the multi-copy Chernoff exponent as a function of the single-copy error probability for any copy-by-copy measurement that

induces a channel approaching a BSC.

We now describe how the quantum fidelity can be used to prove the multi-copy sub-optimality of certain copy-by-copy measurements. In the Supplementary Material, we use a fidelity-based lower bound on  $P_{\epsilon, \min}^{(1)}$  [25] to upper bound the Chernoff exponent of any copy-by-copy measurement via

$$\begin{aligned} \xi^{\text{Meas}} &\leq -\frac{1}{2} \ln (F(\rho_1, \rho_2)) \\ &+ \frac{G\left(\frac{1}{2}\left[1 - \sqrt{1 - F(\rho_1, \rho_2)}\right]\right)}{\sqrt{F(\rho_1, \rho_2)}} b^2 + O(b^4). \end{aligned} \quad (4)$$

where the bias parameter  $b$  can be identified for a given measurement on a case-by-case basis. Crucially, for pure-vs-mixed state discrimination, the QCB is known to be given by  $\xi^{\text{QCB}} = -\ln (F(\rho_1, \rho_2))$  [22], where the fidelity becomes  $F(\rho_1, \rho_2) = \langle \psi_1 | \rho_2 | \psi_1 \rangle$  when one of the states  $\rho_1 = |\psi_1\rangle\langle\psi_1|$  is pure. Therefore, Eq. (4) reveals that, for an arbitrary pure-vs-mixed state discrimination task, any measurement that induces a BSC for each copy of the received state will exhibit a Chernoff exponent that falls below the QCB by a gap of *at least* a factor of two, that is,

$$\xi^{\text{Meas}} \leq \frac{1}{2} \xi^{\text{QCB}} + O(b^2). \quad (5)$$

We show in the Supplementary Material that the Helstrom measurement for coherent-vs-thermal state discrimination exhibits  $b = 0$  in the photon-starved limit  $\bar{n}_S \rightarrow 0$ , satisfying the unbiased criterion for a BSC. This proves that the quantum-optimal copy-by-copy measurement will be strictly sub-optimal in its multi-copy error exponent by at least a factor of two; in the Supplementary Material we analytically show that the gap between the Helstrom measurement and the QCB is in fact exactly a factor of four in the photon-starved limit [13].

Eq. (4) also reveals the role of the bias parameter  $b$  for the Chernoff exponents of copy-by-copy measurements. Note that the  $b^2$  term in both Eqs. (4) and (5) will be strictly positive because of the positivity of the  $G(x)$  function. This means that introducing a small amount of bias in a binary measurement necessarily *increases* the upper bound on the Chernoff exponent, allowing the enforced gap with respect to the QCB to possibly *decrease* to less than a factor of two. We conclude that, for any pure-vs-mixed state discrimination task, bias in the induced conditional error probabilities is a *necessary* criterion for the error decay rate of any copy-by-copy measurement to break free from two-fold sub-optimality and approach toward the QCB. For coherent-vs-thermal state discrimination, we show in the Supplementary Material that a GK measurement that makes a hard decision after each received copy (which can be implemented with ON/OFF detectors) exhibits a bias of  $b = (2 - \sqrt{e})/\sqrt{e} \approx 0.2131$  in the photon-starved limit,

and the resulting upper bound on  $\xi^{\text{GK}}$  from Eq. (4) indicates a gap with respect to the QCB of at least a factor of  $(8\sqrt{e} - 8)/e \approx 1.9092$  [26]. The performance of the GK measurement for coherent-vs-thermal state discrimination is again confirmed to be *nearly* equivalent to that of the Helstrom measurement [19], but the small amount of bias in the measurement allows for a small decrease in the factor of sub-optimality. On the other hand, the Kennedy receiver is fully biased with  $b = 1$  and is able to exactly achieve  $\xi^{\text{KEN}} = \xi^{\text{QCB}}$ . The Chernoff exponents shown in Fig. 3 visualize the role of measurement bias as a necessary ingredient for a receiver to approach the quantum-optimal multi-copy error rate for pure-vs-mixed state discrimination.

Operation of the Kennedy receiver requires a priori knowledge of both the phase and amplitude of the received signal under the coherent state hypothesis. Such an assumption makes this receiver most relevant for an active sensing scenario such as laser target detection or ranging. Additionally, important work is being pursued developing receivers which use coherent displacement that are robust to realistic noise channels requiring the phase of the received signal to be tracked [27].

Research at USC was sponsored by the Army Research Office and was accomplished under Grant Number W911NF-20-1-0235. MG and SG acknowledge support from the DARPA IAMBIC Program under contract number HR00112090128. The views and conclusions contained in this document are those of the authors and should not be interpreted as representing the official policies, either expressed or implied, of the Army Research Office, DARPA or the U.S. Government. The U.S. Government is authorized to reproduce and distribute reprints for Government purposes notwithstanding any copyright notation herein.

---

- [1] C. Wittmann, M. Takeoka, K. N. Cassemiro, M. Sasaki, G. Leuchs, and U. L. Andersen, Demonstration of near-optimal discrimination of optical coherent states, *Physical Review Letters* **101**, 210501 (2008).
- [2] S. Dolinar, An optimal receiver for the binary coherent state quantum channel, *MIT Quarterly Progress Report* **111**, 115 (1973).
- [3] R. L. Cook, P. J. Martin, and J. M. Geremia, Optical coherent state discrimination using a closed-loop quantum measurement, *Nature* **446**, 774 (2007).
- [4] R. S. Kennedy, A near-optimum receiver for the binary coherent-state quantum channel, *MIT Research Laboratory for Electronics Quarterly Progress Report* **110**, 219 (1972).
- [5] M. T. DiMario and F. E. Becerra, Robust measurement for the discrimination of binary coherent states, *Phys. Rev. Lett.* **121**, 023603 (2018).
- [6] S. Guha, J. L. Habif, and M. Takeoka, Approaching helstrom limits to optical pulse-position demodulation using

single photon detection and optical feedback, *Journal of Modern Optics* **58**, 257 (2011).

[7] J. Chen, J. L. Habif, Z. Dutton, R. Lazarus, and S. Guha, Optical codeword demodulation with error rates below the standard quantum limit using a conditional nulling receiver, *Nature Photonics* **6**, 374 (2012).

[8] F. Becerra, J. Fan, G. Baumgartner, J. Goldhar, J. Kosloski, and A. Migdall, Experimental demonstration of a receiver beating the standard quantum limit for multiple nonorthogonal state discrimination, *Nature Photonics* **7**, 147 (2013).

[9] S. Izumi, M. Takeoka, K. Ema, and M. Sasaki, Quantum receivers with squeezing and photon-number-resolving detectors for m-ary coherent state discrimination, *Physical Review A* **87**, 042328 (2013).

[10] A. Ferdinand, M. DiMario, and F. Becerra, Multi-state discrimination below the quantum noise limit at the single-photon level, *npj Quantum Information* **3**, 1 (2017).

[11] R. Nair, S. Guha, and S.-H. Tan, Realizable receivers for discriminating coherent and multicity quantum states near the quantum limit, *Phys. Rev. A* **89**, 032318 (2014).

[12] K. M. R. Audenaert, J. Calsamiglia, R. Munoz-Tapia, E. Bagan, L. Masanes, A. Acin, and F. Verstraete, Discriminating states: The quantum chernoff bound, *Physical Review Letters* **98** (2016).

[13] J. L. Habif and S. Guha, Quantum-limited discrimination between laser light and noise, in *Laser Science* (Optical Society of America, 2018) pp. LM1B-2.

[14] X.-M. Lu, H. Krovi, R. Nair, S. Guha, and J. H. Shapiro, Quantum-optimal detection of one-versus-two incoherent optical sources with arbitrary separation, *npj Quantum Information* **4**, 1 (2018).

[15] Q. Zhuang, Z. Zhang, and J. H. Shapiro, Optimum mixed-state discrimination for noisy entanglement-enhanced sensing, *Physical review letters* **118**, 040801 (2017).

[16] L. Cohen, E. S. Matekole, Y. Sher, D. Istrati, H. S. Eisenberg, and J. P. Dowling, Thresholded quantum lidar: Exploiting photon-number-resolving detection, *Physical Review Letters* **123**, 203601 (2019).

[17] L. Cohen and M. M. Wilde, Towards optimal quantum ranging–hypothesis testing for an unknown return signal, *arXiv preprint arXiv:2109.01601* (2021).

[18] C. You, M. A. Quiroz-Juárez, A. Lambert, N. Bhusal, C. Dong, A. Perez-Leija, A. Javaid, R. d. J. León-Montiel, and O. S. Magaña-Loaiza, Identification of light sources using machine learning, *Applied Physics Reviews* **7**, 021404 (2020).

[19] J. L. Habif, A. Jagannathan, S. Gartenstein, P. Amory, and S. Guha, Quantum-limited discrimination of laser light and thermal light, *Optics Express* **29**, 7418 (2021).

[20] H. L. Van Trees and K. Bell, *Detection Estimation and Modulation Theory, Part I: Detection, Estimation, and Filtering Theory*, 2nd ed. (John Wiley & Sons, Hoboken, New Jersey, 2013).

[21] M. Nussbaum and A. Szkola, The Chernoff lower bound for symmetric quantum hypothesis testing, *Annals of Statistics* **37**, 10.1214/08-AOS593 (2009).

[22] V. Kargin *et al.*, On the chernoff bound for efficiency of quantum hypothesis testing, *Annals of statistics* **33**, 959 (2005).

[23] S. B. Alexander, *Optical communication receiver design*, 37 (IET, 1997).

[24] C. W. Helstrom, *Quantum Detection and Estimation Theory*, 1st ed. (Academic Press, New York NY, 1976).

[25] C. A. Fuchs and J. Van De Graaf, Cryptographic Distinguishability Measures, *IEEE Transactions on Information Theory* **45**, 1216 (1999).

[26] See Table S1 in the Supplementary Material for analytical comparison of the Chernoff exponents  $\xi^{\text{KEN}}$ ,  $\xi^{\text{GK}}$ ,  $\xi^{\text{Helstrom}}$ , and  $\xi^{\text{DD}}$  in the photon-starved limit.

[27] M. T. DiMario and F. E. Becerra, Phase tracking for sub-shot-noise-limited receivers, *Phys. Rev. Research* **2**, 023384 (2020).

[28] M. M. Wilde, *Quantum information theory* (Cambridge University Press, 2013).

[29] A. Acín, E. Bagan, M. Baig, L. Masanes, and R. Muñoz-Tapia, Multiple-copy two-state discrimination with individual measurements, *Physical Review A - Atomic, Molecular, and Optical Physics* **71**, 1 (2005).

[30] L. Banchi, S. L. Braunstein, and S. Pirandola, Quantum Fidelity for Arbitrary Gaussian States, *Physical Review Letters* **115**, 1 (2015), arXiv:1507.01941.

[31] M. R. Grace and S. Guha, Perturbation Theory for Quantum Information, arXiv:2106.05533 (2021).

[32] R. M. Gagliardi and S. Karp, *Optical communications* (Wiley New York, 1976).

[33] A. E. Lita, A. J. Miller, and S. W. Nam, Counting near-infrared single-photons with 95% efficiency, *Opt. Express* **16**, 3032 (2008).

## Asymptotic Sub-Optimality of Optimal Copy-By-Copy Measurements

In the supplement, we consider binary quantum hypothesis tests between arbitrary mixed quantum states  $\rho_1$  and  $\rho_2$  on a Hilbert space  $\mathcal{H}$  and show that a fundamental gap exists between the asymptotic error exponent achieved by certain relevant copy-by-copy measurements and the ultimate asymptotic error rate. In particular, we consider all decision schemes that act the same measurement on each copy of the received state  $\rho_R$  and perform a post-processing procedure that yields a hard decision following each copy. Such measurement schemes, which can be modeled by a two-element POVM, induce a binary-input-binary-output statistical channel consisting of two possible single-copy outcomes  $\rho_1$  and  $\rho_2$  associated with two candidate hypotheses.

Let the conditional probabilities associated with a single-copy error be  $p = P^{(1)}(\rho_2|\rho_1)$  and  $q = P^{(1)}(\rho_2|\rho_2)$ , such that the average probability of making an error on a single copy is  $P_\epsilon^{(1)} = (p+q)/2$ , assuming equal prior probabilities. The classical Chernoff exponent for such a measurement is given by  $\xi^{\text{Meas}} = -\ln(Q_{s_{\min}})$ , where  $Q_{s_{\min}} = \min_{0 \leq s \leq 1} Q_s$  and [20]

$$Q_s = (1-p)^s q^{1-s} + p^s (1-q)^{1-s}. \quad (6)$$

Since the quantity to be minimized is strictly concave [12], solving for  $s$  gives the unique minimum

$$s_{\min} = \frac{\ln((1-q)\ln(\frac{1-q}{p})) - \ln(q\ln(\frac{1-p}{q}))}{\ln(\frac{(1-p)(1-q)}{pq})}. \quad (7)$$

We now parameterize the two single-copy error probabilities  $p = (1+b)P_\epsilon^{(1)}$  and  $q = (1-b)P_\epsilon^{(1)}$  using a quantity  $b \in [-1, 1]$  that quantifies the bias of the total average error toward either  $p$  or  $q$ . In particular, the unbiased condition  $b = 0$  (i.e.,  $p = q = P_\epsilon^{(1)}$ ) implies that the measurement induces a Binary Symmetric Channel (BSC). Expanding  $Q_{s_{\min}}$  around  $b = 0$ , we find Eq. (3) from the main text, where

$$G(P_\epsilon^{(1)}) = \exp\left(\frac{\ln(\bar{P}_\epsilon)^2 - \ln(P_\epsilon^{(1)})^2}{2(\ln(\bar{P}_\epsilon) - \ln(P_\epsilon^{(1)}))}\right) \frac{\left(\bar{P}_\epsilon^2 + 2\tanh^{-1}(\bar{P}_\epsilon)((\bar{P}_\epsilon + 2(P_\epsilon^{(1)})^2)\tanh^{-1}(\bar{P}_\epsilon) - \bar{P}_\epsilon)\right)}{\bar{P}_\epsilon^2 \ln(P_\epsilon^{(1)}/\bar{P}_\epsilon)} \quad (8)$$

is a strictly positive function on the domain  $P_\epsilon^{(1)} \in [0, 1/2]$ , while  $\bar{P}_\epsilon = 1 - P_\epsilon^{(1)}$  and  $\bar{P}_\epsilon = 1 - 2P_\epsilon^{(1)}$ .

We next write the series of inequalities

$$\begin{aligned} Q_{s_{\min}} &\geq 2\sqrt{P_{\epsilon,\min}^{(1)}(1 - P_{\epsilon,\min}^{(1)})} - G(P_{\epsilon,\min}^{(1)})b^2 + O(b^4) \\ &\geq \sqrt{F(\rho_1, \rho_2)} - G\left(\frac{1}{2}\left[1 - \sqrt{1 - F(\rho_1, \rho_2)}\right]\right)b^2 + O(b^4). \end{aligned} \quad (9)$$

The first inequality in Eq. (9) is the Helstrom bound  $P_\epsilon^{(1)} \geq P_{\epsilon,\min}^{(1)}$  on the average error of any hypothesis test between two quantum states  $\rho_1$  and  $\rho_2$ , where  $P_{\epsilon,\min}^{(1)} = \frac{1}{2}(1 - \frac{1}{2}\|\rho_1 - \rho_2\|_1)$  and where  $\|\cdot\|_1$  indicates the operator trace norm [24, 28]; the second inequality is from the well known result of Fuchs and van de Graaf [25],

$$1 - \sqrt{F(\rho_1, \rho_2)} \leq \|\rho_1 - \rho_2\|_1 \leq \sqrt{1 - F(\rho_1, \rho_2)}, \quad (10)$$

where  $F(\rho_1, \rho_2) = \text{Tr}[\sqrt{\sqrt{\rho_1}\rho_2\sqrt{\rho_1}}]^2$  is the quantum fidelity between quantum states. Monotonicity is also used in both inequalities in Eq. (9), as  $\sqrt{x(1-x)}$  monotonically increases on  $x \in [0, 1/2]$  and  $G(x)$  monotonically decreases on  $x \in [0.1166, 1/2]$ . Taylor expanding the logarithm in the definition  $\xi^{\text{Meas}} = -\ln(Q_{s_{\min}})$ , Eq. (4) from the main text is an upper bound on the Chernoff exponent for any copy-by-copy measurement for any quantum state discrimination task. We can additionally lower bound the Chernoff exponent for the specific choice of the Helstrom measurement, which always consists of a two-element POVM and attains the fundamental minimum single-copy error probability  $P_{\epsilon,\min}^{(1)}$  [24]. Using the lower bound in Eq. (10), we find

$$\begin{aligned} \xi^{\text{Helstrom}} &\geq -\frac{1}{2}\ln\left(\sqrt{F(\rho_1, \rho_2)}(2 - \sqrt{F(\rho_1, \rho_2)})\right) \\ &\quad + O(b^2). \end{aligned} \quad (11)$$

We now compare the classical Chernoff exponent for the Helstrom measurement against the quantum Chernoff exponent in three general scenarios spanning all binary quantum hypothesis tests. First, when  $\rho_1 = |\psi_1\rangle\langle\psi_1|$  and  $\rho_2 = |\psi_2\rangle\langle\psi_2|$  are both pure states, the quantum Chernoff exponent is exactly given by [22]

$$\xi^{\text{QCB}} = -\ln(F(\rho_1, \rho_2)), \quad (12)$$

where  $F(\rho_1, \rho_2) = |\langle\psi_1|\psi_2\rangle|^2$  for two pure states. For pure states, the Helstrom measurement is defined by two linear projectors  $|v_1\rangle = (|0\rangle + |1\rangle)/\sqrt{2}$  and  $|v_2\rangle = (|0\rangle - |1\rangle)/\sqrt{2}$  on the 2D subspace of  $\mathcal{H}$  spanned by the two candidate states, where the basis vectors are given by  $|0\rangle = (|\psi_1\rangle + |\psi_2\rangle)/(\sqrt{2}(1 + \text{Re}(\langle\psi_1|\psi_2\rangle)))$  and  $|1\rangle = (|\psi_1\rangle - |\psi_2\rangle)/(\sqrt{2}(1 - \text{Re}(\langle\psi_1|\psi_2\rangle)))$ . It is simple to show that the conditional error probabilities  $p = |\langle v_2|\psi_1\rangle|^2$  and  $q = |\langle v_1|\psi_2\rangle|^2$  are both given by  $p = q = (1 + \sqrt{1 - \text{Re}(\langle\psi_1|\psi_2\rangle)^2})/(2 - 2\text{Re}(\langle\psi_1|\psi_2\rangle)^2)$ , proving that the Helstrom measurement for pure states always induces a BSC, i.e.,  $b = 0$ . From this observation, along with the fact that pure states saturate the upper bound in Eq. (10) [24], we have  $\xi^{\text{Helstrom}} = -(1/2)\ln(F(\rho_1, \rho_2))$ , confirming the known fact that the Helstrom measurement, which is quantum-optimal for single-copy discrimination, achieves an asymptotic error exponent that is sub-optimal by *exactly* a factor of two compared with the asymptotic quantum limit for multi-copy discrimination [29].

When  $\rho_1 = |\psi_1\rangle\langle\psi_1|$  is a pure state and  $\rho_2$  is a mixed state, the quantum Chernoff exponent is again known to be given by Eq. (12), where  $F(\rho_1, \rho_2) = |\langle\psi_1|\rho_2|\psi_1\rangle|^2$  [22]. The most general description of the Helstrom measurement involves the eigenspectrum of the operator  $\Lambda = \rho_1 - \rho_2$ ; the measurement projectors  $\Pi_1^{\text{Helstrom}}$  and  $\Pi_2^{\text{Helstrom}}$  are defined as the subspaces on  $\mathcal{H}$  corresponding to positive and negative eigenvalues of  $\Lambda$ , respectively [24]. The resulting conditional error probabilities  $p = \text{Tr}[\Pi_2^{\text{Helstrom}}\rho_1]$  and  $q = \text{Tr}[\Pi_1^{\text{Helstrom}}\rho_2]$  do not in general approach the BSC condition  $p = q = P_\epsilon^{(1)}$ , although we will show that the unbiased condition is satisfied for the experimental discrimination task discussed in the main text. From Eq. (4) in the main text and Eq. (12) (which holds when  $\rho_1$  and/or  $\rho_2$  is pure), we conclude that any measurement that does induce a channel that approaches a BSC (to first order in  $b$ ) exhibits an asymptotic error exponent that is *at least* a factor of two lower than the quantum Chernoff exponent for pure-vs-mixed state hypothesis testing, as in Eq. (5) in the main text.

When  $\rho_1$  and  $\rho_2$  are both mixed states, Eq. (4) in the main text still holds, while the quantum Chernoff exponent cannot be exactly determined in terms of the fidelity but is known to obey the bounds [22]

$$-\frac{1}{2}\ln(F(\rho_1, \rho_2)) \leq \xi^{\text{QCB}} \leq -\ln(F(\rho_1, \rho_2)). \quad (13)$$

To first order in  $b$ , the bounded intervals for  $\xi^{\text{Meas}}$  and  $\xi^{\text{QCB}}$  intersect at exactly the point  $-(1/2)\ln(F(\rho_1, \rho_2))$ , meaning that we cannot show a gap between the quantum and classical Chernoff exponents; rather, we simply reaffirm that  $\xi^{\text{Meas}} \leq \xi^{\text{QCB}}$ , which is the operational meaning of the quantum Chernoff bound [12, 21]. It is possible that restricting the states further, for example by considering only Gaussian states [30] or states that are separated by a vanishingly small operator perturbation [31], could lead to a tighter lower bound on the QCB and reveal a gap between BSC-inducing measurements and the quantum limit, but we leave this for future work.

### Asymptotic Receiver Performance for Coherent vs Thermal State Discrimination

Finally, we analytically investigate the relationship between the asymptotic error exponents of measurement schemes optimized for single-copy and multi-copy discrimination for the example of discriminating between  $M$  copies of a coherent state  $\rho_{\text{th}}^{\otimes M}$  and a thermal state  $\rho_{\text{coh}}^{\otimes M}$  in the limit  $\bar{n}_S \rightarrow 0$ , when each individual copy of the received state is photon-starved. We first consider the Kennedy measurement characterized by POVM elements  $\Pi_1^{\text{Kennedy}} = \mathcal{I} - \rho_{\text{coh}}$  and  $\Pi_2^{\text{Kennedy}} = \rho_{\text{coh}}$ , where  $\mathcal{I}$  is the identity operator on  $\mathcal{H}$ . Note that for the Kennedy measurement,  $p = \text{Tr}[\rho_{\text{coh}}\rho_{\text{th}}]$  and  $q = 0$ , so  $b = 1$ . Since  $\rho_{\text{coh}}$  is a pure state, the Chernoff exponent  $\xi^{\text{Kennedy}}$  is guaranteed to be equal to the quantum Chernoff exponent  $\xi^{\text{QCB}} = -\ln(F(\rho_{\text{coh}}, \rho_{\text{th}}))$  [22]. The fidelity between the two states is easily calculated in the Fock basis as  $F(\rho_{\text{coh}}, \rho_{\text{th}}) = \text{Tr}[\rho_{\text{coh}}\rho_{\text{th}}] = (1 + \bar{n}_R)^{-1} \exp(-\bar{n}_R/(1 + \bar{n}_R))$ , yielding Eq. 2 in the main text and the photon-starved behavior

$$\xi^{\text{Kennedy}} = \xi^{\text{QCB}} = 2\bar{n}_R + O(\bar{n}_R^2) \quad (14)$$

for the optimal multi-copy asymptotic error rate. On the other hand, when  $P_{\epsilon, \text{min}}^{(1)} > 0.1166$ , which will be true in the limit  $\bar{n}_R \rightarrow 0$ , we can use the fidelity along with Eq. (9) and the first order expansion  $\ln(1 + x) = x + O(x^2)$  to upper

bound the Chernoff exponent for any copy-by-copy measurement:

$$\xi^{\text{Meas}} \leq \left(1 + b^2 + O(b^4)\right) \left(\bar{n}_R + O(\bar{n}_R^2)\right). \quad (15)$$

To analyze specific measurements in the  $\bar{n}_R \rightarrow 0$  limit, we truncate  $\rho_{\text{coh}}$  and  $\rho_{\text{th}}$  to the two-dimensional subspace of  $\mathcal{H}$  corresponding to 0- and 1-photon support in the Fock basis, effectively modeling each state as a qubit. This truncation of the Hilbert space is justified because both states converge to single-mode vacuum in the photon-starved limit. On this subspace, the Helstrom measurement projectors  $\Pi_1^{\text{Helstrom}}$  and  $\Pi_2^{\text{Helstrom}}$  yield the conditional error probabilities  $p = 1/2 + O(\bar{n}_R)$  and  $q = 1/2 - \sqrt{\bar{n}_R} + O(\bar{n}_R)$ . The resulting error allocation parameter is  $b = \sqrt{\bar{n}_R} + O(\bar{n}_R)$ , meaning that the channel induced by the Helstrom measurement for coherent state vs thermal state discrimination converges to a BSC in the photon-starved limit. Using Eq. (15), the Chernoff exponent for the Helstrom measurement must obey the upper bound

$$\xi^{\text{Helstrom}} \leq \bar{n}_R + O(\bar{n}_R^2), \quad (16)$$

enforcing a sub-optimality of at least a factor of two compared with the QCB. Using the conditional error probabilities  $p$  and  $q$ , we find that  $Q_s = 1 - 2s(1 - s)\bar{n}_R + O(\bar{n}_R^2)$ , so to first order in  $\bar{n}_R$  we have  $s_{\min} = 1/2$ . We find that the Helstrom measurement Chernoff exponent

$$\xi^{\text{Helstrom}} = \frac{\bar{n}_R}{2} + O(\bar{n}_R^2) \quad (17)$$

for coherent vs thermal state discrimination does satisfy the sub-optimality of at least a factor of two, as the true gap is a factor of four in the limit of small signal power.

For the GK measurement, we consider the two POVM elements  $\Pi_1^{\text{GK}}$  and  $\Pi_2^{\text{GK}}$  corresponding to ON/OFF photodetection after the coherent displacement. The conditional probabilities are the probability of detecting one or more photons from a coherent state displaced by  $\beta \in \mathbb{R}$ ,  $p = 1 - \exp(-(\sqrt{\bar{n}_R} - \beta)^2)$  and the probability of detecting zero photons from a displaced single-mode thermal state,  $q = (1 + \bar{n}_R)^{-1} \exp(-\beta^2/(1 + \bar{n}_R))$  [32]. Solving for the displacement strength that minimizes the average error  $P_\epsilon^{(1)}$ , the optimum is at exactly  $\beta = 1/\sqrt{2}$  in the limit  $\bar{n}_R \rightarrow 0$ , so we use this choice of displacement in our analysis of the GK receiver in the small signal power limit. The conditional error probabilities become  $p = 1/\sqrt{e} - \bar{n}_R/(2\sqrt{e}) + O(\bar{n}_R^{3/2})$  and  $q = 1 - 1/\sqrt{e} - \sqrt{2\bar{n}_R/e} + O(\bar{n}_R^{3/2})$  and result in  $b = (\sqrt{e} - 2)/\sqrt{e} - 2\sqrt{2\bar{n}_R/e} + O(\bar{n}_R)$ , meaning that the GK measurement does not induce an approximate BSC. Nonetheless, with this value of  $b$  and the minimum error probability  $P_{\epsilon, \min}^{(1)}$ , we use Eqs. (6) and (7) to find that the Chernoff exponent of the GK measurement must be bounded from above according to

$$\xi^{\text{GK}} \leq \frac{e\bar{n}_R}{4(\sqrt{e} - 1)} + O(\bar{n}_R^{3/2}). \quad (18)$$

Since  $e/(4(\sqrt{e} - 1)) = 1.0476$ , the gap between the optimal multi-copy measurement and the copy-by-copy GK receiver must be at least a factor of  $(2\bar{n}_R)/(1.0476\bar{n}_R) = 1.9092$  in the photon-starved limit. This gap is almost identical to the enforced sub-optimality of the Helstrom measurement, but we find that the bias in the GK measurement allows for the gap to be less than a factor of two.

$$\xi^{\text{GK}} = \frac{\bar{n}_R}{4(\sqrt{e} - 1)} + O(\bar{n}_R^{3/2}), \quad (19)$$

where  $1/(4(\sqrt{e} - 1)) = 0.3854$ . The GK receiver obeys the required upper bound on the Chernoff exponent, and its Chernoff exponent is lower than that of the Helstrom measurement.

Finally, we consider direct detection with full PNR detection, i.e., directly measuring in the Fock basis. Directly computing the Chernoff exponent [20], we find that  $Q_s = 1 - (1 - 2^{-s} + s/2)\bar{n}_R^2 + O(\bar{n}_R^3)$ , which in the lowest order in  $\bar{n}_R$  has its minimum at  $s_{\min} = \log(\ln(4)) = 0.4712$ , where  $\log(\cdot)$  is the base 2 logarithm. The resulting Chernoff exponent is

$$\xi^{\text{Direct}} = \frac{1 - \log[\ln(2^e)]}{2} \bar{n}_R^2 + O(\bar{n}_R^3), \quad (20)$$

where the lowest order term equates to  $0.0430\bar{n}_R^2$ . Direct imaging exhibits an inferior scaling behavior with respect to  $\bar{n}_R$  compared with the quantum limit and all three other analyzed receivers as  $\bar{n}_R \rightarrow 0$  (Fig. 3). Table I summarizes the Chernoff exponent calculations for each of these measurements.

| Measurement             | $\xi$  |
|-------------------------|--|
| QCB/Kennedy             | $2\bar{n}_R + O(\bar{n}_R^2)$                            |
| Helstrom (Upper Bound)  | $\bar{n}_R + O(\bar{n}_R^2)$                             |
| Helstrom                | $\frac{\bar{n}_R}{2} + O(\bar{n}_R^2)$                   |
| ON/OFF GK (Upper Bound) | $\frac{e\bar{n}_R}{4(\sqrt{e}-1)} + O(\bar{n}_R^{3/2})$  |
| Direct Detection        | $\frac{1-\log[\ln(2^e)]}{2}\bar{n}_R^2 + O(\bar{n}_R^3)$ |

TABLE I. Analytical forms for the Chernoff exponents of several measurements for  $M$ -copy coherent state vs thermal state discrimination to lowest nonzero order in the mean photon number  $\bar{n}_R$ .

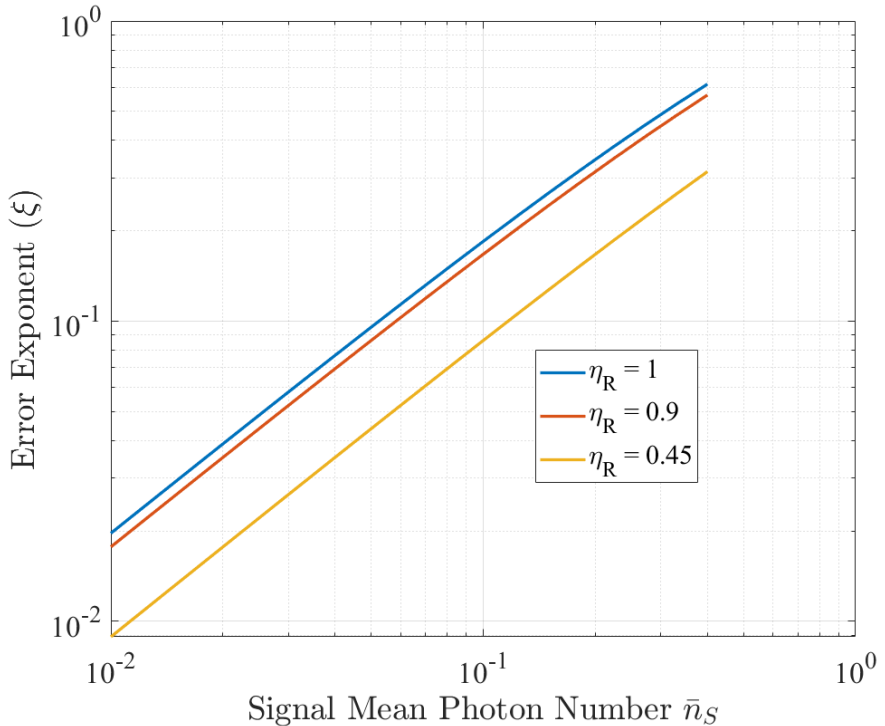


FIG. 4. The error exponent achieved by the Kennedy receiver for three different values of receiver efficiency  $\eta_R$ . When  $\eta_R = 1$  the Kennedy receiver achieves the quantum Chernoff error exponent.

#### Impact of sub-unit receiver efficiency on $\xi^{\text{KEN}}$

In the main text we identified that our laboratory receiver implementation suffered from optical losses which can be attributed to non-idealities in the optical paths within the receiver but is dominated by low detection efficiency in the Silicon SPAD photon counting detector. These effects combined to result in an overall receiver efficiency  $\eta_R = 0.45$ . As our experiment was reported we normalized the intensity of our received state relative to this efficiency. Here we quantify the impact of receiver efficiency on the error exponent for the Kennedy receiver.

Figure 4 shows the error exponent  $\xi^{\text{KEN}}$  for two different values of  $\eta_R$ , compared against the value achieved with an ideal receiver. With our measured receiver efficiency  $\eta_R = 0.45$  the resulting error exponent closely matches that achieved with the unit efficiency generalized Kennedy receiver (reported in the main text). A more appropriate comparison is provided by assuming that our experiment uses state-of-the-art superconducting nanowire single photon detectors with efficiencies  $\eta_R \geq 0.9$  [33].

### The quasi photon number resolving (qPNR) detector

While we do not have a true photon number resolving detector available for the experiment, we approximated such a detector using time resolved photon measurements in a single photon detector with post-processing to achieve a *quasi*-photon number resolving (qPNR) detector. Described in [19], the qPNR was implemented by making time-resolved measurements of single photon events within a  $1 \mu s$  measurement window. A Perkin-Elmer Si avalanche photodiode SPD (SPCM-AQR-14) was used to count photon detection events. The minimum detection time (accounting for detector dead time) for this detector is 50 ns. In the limit that the probability of more than one photon being detected within a 50 ns time window is extremely low then a detection event can be well approximated as a projection onto the  $|n = 1\rangle$  Fock basis state. Summing the detection events within the  $1 \mu s$  interval reports the number of detected photons within the interval.